

understanding of the tropical atmosphere must be of the highest priority, including assessing and improving the quality of regional SST projections in global climate models.

References and Notes

1. C. D. Hoyos, P. A. Agudelo, P. J. Webster, J. A. Curry, *Science* **312**, 94 (2006).
2. K. Emanuel, *J. Climate* **20**, 5497 (2007).
3. U.S. Climate Change Science Program, *Weather and Climate Extremes in a Changing Climate*, T. R. Karl *et al.*, Eds. (Department of Commerce, NOAA's National Climatic Data Center, Washington, DC, 2008).
4. K. L. Swanson, *Geochim. Geophys. Res.* **9**, Q04V01; 10.1029/2007GC001844 (2008).
5. G. A. Vecchi, B. J. Soden, *Nature* **450**, 1066 (2007).
6. PDI is the cube of the instantaneous tropical cyclone wind speed integrated over the life of all storms in a given season; more intense and frequent basinwide hurricane activity lead to higher PDI values.
7. We use 24 different global climate models run in support of the Intergovernmental Panel on Climate Change Fourth Assessment Report (IPCC-AR4) (17). See Supporting Online Material for details.
8. T. R. Knutson *et al.*, *Nature Geosci.* **1**, 359 (2008).
9. R. Zhang, T. L. Delworth, *Geophys. Res. Lett.* **33**, L17712 (2006).
10. D. J. Vimont, J. P. Kossin, *Geophys. Res. Lett.* **34**, L07709 (2007).
11. M. Latif, N. Keenlyside, J. Bader, *Geophys. Res. Lett.* **34**, L01710 (2007).
12. K. A. Emanuel, R. Sundararajan, J. Williams, *Bull. Am. Met. Soc.* **89**, 347 (2008).
13. K. Oouchi *et al.*, *J. Met. Soc. Japan* **84**, 259 (2006).
14. L. Bengtsson *et al.*, *Tellus* **59A**, 539 (2007).
15. B. Santer *et al.*, *Proc. Natl. Acad. Sci. U.S.A.*; 10.1073/pnas.0602861103 (2008).
16. T. R. Knutson *et al.*, *J. Climate* **19**, 1624 (2006).
17. G. A. Meehl *et al.*, *Bull. Am. Meteorol. Soc.* **88**, 1549 (2007).
18. We are grateful for comments from T. Delworth, I. Held, S. Ilcane, A. Johansson, T. Knutson, D. E. Harrison, and M. Vecchi. This work was partly supported by NOAA/OGP.

Supporting Online Material

www.sciencemag.org/cgi/content/full/322/5902/687/DC1
Materials and Methods
SOM Text
Figs. S1 to S8
References

10.1126/science.1164396

MATERIALS SCIENCE

Nanoscale Polymer Processing

Christopher L. Soles¹ and Yifu Ding²

It is difficult to find a manufactured object that does not contain at least some polymeric (plastic) components. This ubiquity reflects the ease with which polymers can be formed into arbitrary shapes through processes that induce flow of a viscous polymer melt into the cavity of a mold or die. The equations that quantify the rheological response of viscous polymer melts under large-scale deformations have been developed over the past 60 years, providing the paradigms by which forming processes are optimized to produce well-controlled, high-quality, robust polymeric parts (1). These paradigms, however, are poised to change as polymer processing approaches the nanoscale. On page 720 of this issue, Rowland *et al.* present evidence suggesting that the relationships that govern the viscous flow of polymers in highly confined geometries are dramatically different from those of the bulk (2).

Nanoimprint lithography (NIL) can be used to manufacture polymeric features with dimensions of 10 nm or smaller (3). The thermal embossing form of NIL relies on a melt squeeze-flow process to transform a smooth polymer film into a patterned surface. Nanoscale features that have been etched into silicon, quartz, or some other hard template material can be inexpensively replicated by stamping the template into a thin polymeric film. Even roll-to-roll NIL tools capable of continuous, high-throughput patterning are

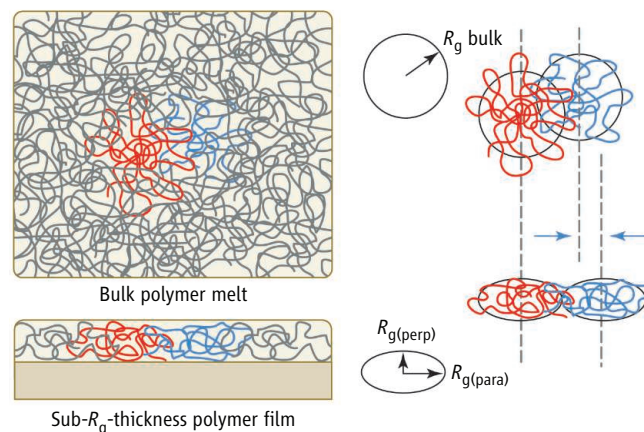
now available (4). However, optimizing such NIL processes will require knowledge of the rheological response of the polymer being squeezed into a nanoscale cavity, as well as the effect of this response on the properties of the imprinted structure (5).

The large-strain deformation properties of a polymer melt are dominated by the topological entanglement of the transient network established by the sea of interpenetrating polymer coils (see the figure). The volume pervaded by a single molecule (proportional to R_g^3 , where R_g is the radius of gyration of a single coil) is nearly an order of magnitude larger than the sum of the hard-core volumes of the atoms that constitute the macromolecular chain. The degree of interpenetration or entanglement between neighboring coils is determined by the pervaded volume of a single macromolecular coil and the packing density of the individual chain segments. The large-scale rheological response of a polymer melt is then determined by the response of this entangled network to an applied load. Both the pervaded volume and the extent of entanglement increase with molecular mass,

The established rules for fabricating plastics now require a rethink as feature sizes of the products head toward the nanoscale.

thereby making the flow of the high-molecular-mass melts more viscous. The rheological consequences of squeezing a polymer into a cavity or dimension that is smaller than the pervaded volume of the molecule itself are not obvious.

Because quantitative rheological measurements in NIL are complicated, Rowland *et al.* designed a simplified method that mimics the large-strain deformation fields encountered. An instrumented indenter records the force and displacement as a well-defined flat punch



Processing polymers. (Upper left) A sea of interpenetrating macromolecular coils in a polymer melt. (Right) An arbitrary pair of nearest-neighbor coils, highlighted in red and blue, is lifted from the melt to illustrate their radius of gyration (R_g) and the fact that interpenetration or entanglement between the coils exists; the separation between the centers of mass between the two coils is less than $2R_g$. (Lower left) For thin films with total thickness below R_g , the coils do not appear to spread laterally, and $R_{g(\text{para})} \approx R_g > R_{g(\text{perp})}$. This implies that the interpenetration of the coils decreases, and as argued by Rowland *et al.*, suggests a loss of entanglement and a decreased resistance to flow in a thin-film polymer melt.

¹Polymers Division, National Institute of Standards and Technology, Gaithersburg, MD 20899, USA. ²Department of Mechanical Engineering, University of Colorado, Boulder, CO 80309, USA. E-mail: csoles@nist.gov

is pressed into a polymer film. The films are monodispersed polystyrenes with average molecular masses of 9000 kD, 900 kD, and 44 kD, with corresponding R_g values of approximately 84 nm, 26 nm, and 6 nm, respectively, in the bulk melt state (R_g scales with the square root of molecular mass). The film thickness, h , is varied from 170 nm to 36 nm, becoming thinner than the R_g of the highest-molecular-mass polystyrenes. The authors argue that the rheological response where the thickness of the film is strongly confining relative to the diameter of the molecule is relevant to an NIL imprint where the mold cavity is smaller than the R_g of the polymer.

The results are striking. For thick films ($h \gg R_g$), the resistance to the large-strain deformation of the polymer melt increases substantially with the molecular mass of the polystyrene, consistent with the bulk viscosity. However, when the film thickness is smaller than the radius of gyration, both the contact modulus (the resistance to small-scale elastic deformation) and the forming stress (the load required to induce large-scale plastic deformation) are strongly reduced. For the polystyrene with the highest molecular mass (9000 kD) in the 36-nm film, which is approximately one-half the bulk R_g , both the forming stress and large-strain deformation resistance are smaller than for the lowest-molecular-mass polystyrene (44 kD) of the same thickness. This thickness is still about 6 times the bulk R_g for the 44-kD polystyrene

and is therefore presumably less confined.

Why such a dramatic reduction of the forming stress and flow resistance in high-molecular-mass polymers relative to the bulk viscosity? The large-strain properties of polymers are dominated by the topological entanglements of the transient network established by the interpenetrating polymer coils (6). For chains at surfaces, at interfaces, and in thin films, it has been suggested that the interface acts as a reflecting plane. The polymer coil is not allowed to cross the boundary, so it must “reflect” and remain within the confines of the interface (7–9). Small-angle neutron scattering measurements on thin polymer films have shown that the R_g in the plane of the film is unaffected by thin-film confinement (10). This means that when the film thickness decreases and starts to compress the coil in the vertical direction, the polymer does not respond by spreading laterally in-plane (see the figure). Rather, the chain folds back on itself at the film interface, resulting in the chain segment’s nearest neighbors belonging to the same chain, thus decreasing the degree of coil-coil interpenetration (11).

These arguments are provocative given the strong correlation between entanglement and melt rheology. A loss of entanglement would seem to facilitate flow in polymer thin films. Although this has been very difficult to prove, the experimental results of Rowland *et al.* provide some of the strongest evidence to date to support this argument. Si and co-workers (12)

used tensile deformation measurement of glassy polystyrene to deduce a loss of entanglement in thin polymer films, which seems to support the reports of facilitated flow here. However, there are also compelling reports from bubble inflation (13) and surface force (14) measurements of polymer melts “stiffening” in very thin films. How this problem unravels is not only a scientifically intriguing question, but is also of technical relevance as manufacturing processes such as NIL evolve to fabricate nanoscale features from relatively gigantic molecules.

References

1. J. D. Ferry, *Viscoelastic Properties of Polymers* (Wiley, New York, ed. 3, 1980).
2. H. D. Rowland, W. P. King, J. B. Pethica, G. L. W. Cross, *Science* **322**, 720 (2008); published online 2 October 2008 (10.1126/science.1157945).
3. S. Y. Chou, P. R. Krauss, P. J. Renstrom, *Science* **272**, 85 (1996).
4. S. H. Ahn, L. J. Guo, *Adv. Mater.* **20**, 2044 (2008).
5. Y. F. Ding *et al.*, *Adv. Mater.* **19**, 1377 (2007).
6. M. S. Green, A. V. Tobolsky, *J. Chem. Phys.* **14**, 80 (1946).
7. E. A. DiMarzio, *J. Chem. Phys.* **42**, 2101 (1965).
8. H. R. Brown, T. P. Russell, *Macromolecules* **29**, 798 (1996).
9. L. J. Fetters, D. J. Lohse, D. Richter, T. A. Witten, A. Zirkel, *Macromolecules* **27**, 4639 (1994).
10. R. L. Jones, S. K. Kumar, D. L. Ho, R. M. Briber, T. P. Russell, *Nature* **400**, 146 (1999).
11. P. G. de Gennes, *Scaling Concepts in Polymer Physics* (Cornell Univ. Press, Ithaca, NY, 1979).
12. L. Si, M. V. Massa, K. Dalnoki-Veress, H. R. Brown, R. A. L. Jones, *Phys. Rev. Lett.* **94**, 4 (2005).
13. P. A. O’Connell, G. B. McKenna, *Science* **307**, 1760 (2005).
14. H. W. Hu, S. Granick, *Science* **258**, 1339 (1992).

10.1126/science.1165174

ECOLOGY

Physiology and Climate Change

Hans O. Pörtner¹ and Anthony P. Farrell²

Ongoing ecosystem changes in response to climate change include poleward or altitudinal shifts in geographical distribution (1–3), population collapses or local extinctions (4), failure of large-scale animal migrations (5), changes in the seasonal timing of biological events (6), and changes in food availability and food web structure. These changes are largely driven by environmental temperature (1, 7). Examples from aquatic animal communities show that study of physiological mechanisms can help to elucidate these ecosystem chan-

ges and to project future ecological trends.

All organisms live within a limited range of body temperatures, due to optimized structural and kinetic coordination of molecular, cellular, and systemic processes. Functional constraints result at temperature extremes. Increasing complexity causes narrower thermal windows for whole-organism functions than for cells and molecules, and for animals and plants than for unicellular organisms (8). Direct effects of climatic warming can be understood through fatal decrements in an organism’s performance in growth, reproduction, foraging, immune competence, behaviors and competitiveness. Performance in animals is supported by aerobic scope, the increase in oxygen consumption rate from resting to maximal (9). Performance falls below its optimum during cooling and

Studies of physiological mechanisms are needed to predict climate effects on ecosystems at species and community levels.

warming. At both upper and lower pejus temperatures, performance decrements result as the limiting capacity for oxygen supply causes hypoxemia (4, 8) (see the figure, left). Beyond low and high critical temperatures, only a passive, anaerobic existence is possible. Fish rarely exploit this anaerobic range, but invertebrates inhabiting the highly variable intertidal environment use metabolic depression, anaerobic energy production, and stress protection mechanisms to provide short- to medium-term tolerance of extreme temperatures.

Thermal windows likely evolved to be as narrow as possible to minimize maintenance costs, resulting in functional differences, between species and subspecies in various climate zones (10–12) and even between populations of a species (13); for example, the

¹Animal Ecophysiology, Alfred-Wegener-Institute for Polar and Marine Research, 27515 Bremerhaven, Germany. E-mail: hans.poertner@awi.de ²Department of Zoology and Faculty of Land and Food Systems, University of British Columbia, Vancouver, V6T 1Z4 Canada.